Interactions between the Three CIN85 SH3 Domains and Ubiquitin: Implications for CIN85 Ubiquitination†

Irina Bezsonova,[‡,§] M. Christine Bruce,[||,⊥] Silke Wiesner,[§,#] Hong Lin,[§] Daniela Rotin,[||,⊥] and Julie D. Forman-Kay*[,§,⊥]

Department of Chemistry, University of Toronto, 80 St. George Street, Toronto, ON, Canada M5S 1A8, Program in Molecular Structure and Function and Program in Cell Biology, Hospital for Sick Children, 555 University Avenue, Toronto, ON, Canada M5G 1X8, and Department of Biochemistry, University of Toronto, 1 King's College Circle, Toronto, ON, Canada M5S 1A8

Received March 14, 2008; Revised Manuscript Received June 13, 2008

ABSTRACT: CIN85 is an adaptor protein linking the ubiquitin ligase Cbl and clathrin-binding proteins in clathrin-mediated receptor endocytosis. The SH3 domains of CIN85 bind to a proline-rich region of Cbl. Here we show that all three SH3 domains of CIN85 bind to ubiquitin. We also present a data-based structural model of the CIN85 SH3-C domain in complex with ubiquitin. In this complex, ubiquitin binds to the canonical interaction surface of the SH3 domain for proline-rich ligands and mimics the PPII helix, and we provide evidence that ubiquitin competes with these ligands for binding. We demonstrate that disruption of ubiquitin binding results in constitutive ubiquitination of CIN85 and an increased level of ubiquitination of EGFR in the absence of EGF stimulation. These results suggest that competition between Cbl and ubiquitin binding to CIN85 regulates Cbl function and EGFR endocytosis.

Activation of receptor tyrosine kinases (RTKs) initiates a cascade of protein−protein interactions that control cellular proliferation and differentiation. The intensity and duration of RTK signaling are regulated by their removal from the cell surface, in a process dependent on receptor ubiquitination and dynamic interaction with accessory endocytic proteins. The activated EGF receptor (EGFR),[1] for example, is monoubiquitinated by the ubiquitin ligase Cbl, targeting the receptor for lysosomal degradation (*1*). Phosphorylation of Cbl by the activated EGFR induces an interaction between Cbl and the adaptor protein CIN85 (Cbl-interacting protein of 85 kDa, also known as Ruk or SETA), which in turn results in the ubiquitination of CIN85 and ultimately mediates receptor internalization through regulatory components of clathrin-coated vesicles such as endophilins (*2, 3*). Once internalized, the EGFR is delivered to endosomal compartments where it may either recycle back to the cell surface or be targeted to the lysosomes for degradation.

The ubiquitin ligase Cbl is a 120 kDa, ubiquitously expressed cytoplasmic protein involved in ligand-induced downregulation of receptor tyrosine kinases. Cbl-mediated ubiquitination of active receptors is essential for receptor degradation and termination of receptor-induced signal transduction (*4*). Cbl consists of an N-terminal tyrosine kinase binding domain (TKB), a short linker region, and a RING finger domain followed by a long carboxyl terminus that is divergent among Cbl family members. In the case of c-Cbl, the C-terminus includes a proline-rich region, an acidic box domain with serine/threonine- and tyrosine-rich stretches, and a leucine zipper domain (LZ) highly similar in sequence to ubiquitin-associated domains (UBA).

CIN85 (human orthologue of yeast Sla1) was identified as a binding partner for the C-terminal region of Cbl (*5*). CIN85 contains three N-terminal Src-homology 3 (SH3) domains, a proline-rich region, and a C-terminal coiled-coil domain. SH3 domains are small (50−70 residues) modular interaction domains that generally bind to a proline-containing targets (PxxP motifs) in a polyproline type II (PPII) helical conformation (*6*). It has been shown that SH3 domains of CIN85 bind to an atypical proline-arginine (PxxxPR) motif in the C-terminus of Cbl. This interaction is dependent on tyrosine phosphorylation of Cbl by EGFR, and it has been suggested that a conformational change occurs upon phosphorylation that exposes and/or stabilizes the Cbl PxxxPR motif (*7, 8*). Several other CIN85 effectors containing PxxxPR motifs have been identified recently (*9*). They include synaptojanin 2B1, SHIP-1, Hip1R, p115RhoGEF, ASAP1, and ARAP3, which interact directly with CIN85 SH3 domains through their PxxxPR motifs. These proteins are implicated in clathrin-mediated receptor endocytosis, receptor recycling, and cytoskeletal rearrangements. The SH3 domains of CIN85 are also involved in interactions with

† This work was supported by funds from the Canadian Cancer Society to J.D.F.-K.

* To whom correspondence should be addressed. E-mail: forman@sickkids.ca. Phone: (416) 813-5358. Fax: (416) 813-5022.

‡ Department of Chemistry, University of Toronto.

§ Program in Molecular Structure and Function, Hospital for Sick Children.

|| Program in Cell Biology, Hospital for Sick Children.

⊥ Department of Biochemistry, University of Toronto.

Current address: Max Planck Institute for Developmental Biology, Tübingen, Germany.

[1] Abbreviations: NMR, nuclear magnetic resonance; RDCs, residual dipolar couplings; PRE, paramagnetic relaxation enhancement; SH3, Src-homology 3; EGF, epithelial growth factor; EGFR, EGF receptor; Cbl, Casitas B-lineage lymphoma ubiquitin ligase; CIN85, Cbl-interacting protein of 85 kDa; Ub, ubiquitin; UBA, ubiquitin-associated domain.

10.1021/bi800439t CCC: $40.75
Published on Web 08/05/2008

various signaling molecules, among them CD2, AIP/Alix, BLNK, and SB-1, which suggests roles for CIN85 in such diverse cellular processes as T-cell receptor clustering, induction of apoptosis in glial cells, and B-cell receptor signaling (*10*). The proline-rich region of CIN85 interacts with additional SH3 domain-containing proteins, coupling it to cytoskeletal rearrangements (p130Cas and cortactin), regulation of Src family kinases (Fyn, Src, and Yes), and regulation of phosphoinositide metabolism (p85 subunit of phosphatidylinositol-3 kinase) (*10–12*). Intramolecular association between the SH3 domains and the proline-rich region of CIN85 may also occur (*13*), as observed for other modular signaling proteins (*14*). The intact C-terminal coiled-coil region of CIN85 is required for Cbl-directed monoubiquitination of CIN85 (*2*) and mediates CIN85 oligomerization, adding another level of complexity in the formation of multiprotein CIN85-associated protein networks (*15, 16*).

Recently, the third SH3 domain of CIN85 (SH3-C) has been shown to interact with ubiquitin, a novel target for an SH3 domain (*17*). Ubiquitin-binding domains or motifs noncovalently bind to ubiquitin. They are generally small domains or motifs (20−150 residues in length) found in enzymes that catalyze ubiquitination or deubiquitination, or in ubiquitin receptors that recognize and interpret signals from ubiquitinated proteins (*18*). Ubiquitin-binding domains or motifs are structurally diverse and include α-helical domains (UIM, CUE, UBA, and GAT), α/β-domains (UEV), and proteins with extended loops that form a ubiquitin-binding interface (NZF motif). Although there are no obvious common topological themes for ubiquitin-binding domains, they all contact an overlapping face on ubiquitin that in most cases includes Ile 44. The SH3 domain is structurally unrelated to any of these ubiquitin-binding domains. In addition, since ubiquitin contains no proline residues on its SH3 domain-binding interface, its interaction with an SH3 domain is a surprising one. The recently published (*19*) solution NMR structure of ubiquitin in complex with the third SH3 domain of Sla1 (Sla1 SH3-3 domain), which is 34% identical in sequence to the CIN85 SH3-C domain, revealed that the ubiquitin-binding surface of the Sla1 SH3-3 domain substantially overlaps with the canonical binding surface for proline-rich ligands. Like other ubiquitin-binding domains, the Sla1 SH3-3 domain engages a hydrophobic patch surrounding Ile 44 of ubiquitin. On the basis of the NMR structure of the complex and mutational analysis (*17*), residue Phe 401 of Sla1 located in the heart of the ubiquitin-binding surface appears to be an important determinant of the binding specificity.

While the structural basis of ubiquitin recognition by SH3 domains has been elucidated, the biological role of such interaction is still unclear. It has been proposed that the SH3 domain−ubiquitin interaction serves as a switch in a network of interactions that control assembly and disassembly of the endocytic and actin-regulating machinery. In this paper, we investigate the effect of ubiquitin binding to CIN85 on EGF-dependent ubiquitination of EGFR and CIN85, and its potential consequences for EGFR endocytosis. We have generated a data-based structural model of the CIN85 SH3-C domain−ubiquitin complex. As found in the structure of the Sla1 SH3-3 domain−ubiquitin complex, the CIN85 SH3-C domain binds to ubiquitin with its classical PxxP binding site despite the lack of a proline-rich sequence in ubiquitin. Also in agreement with the Sla1 SH3 domain complex, ubiquitin binds to the CIN85 SH3-C domain via a hydrophobic patch having Ile 44 in its center, a surface involved in most ubiquitin protein interactions. However, unlike the yeast Sla1 that binds to ubiquitin with its third SH3 domain only, our NMR titrations reveal that all three SH3 domains (SH3-A, -B, and -C) of CIN85 bind to ubiquitin. We also present evidence that binding of CIN85 to ubiquitin is important for the regulation of EGF-dependent ubiquitination of CIN85. Specifically, we find that preventing CIN85 from binding ubiquitin results in a loss of EGF sensitivity and constitutive ubiquitination of CIN85, as well as an increased level of ubiquitination of EGFR.

MATERIALS AND METHODS

Sample Preparation. The nucleotide sequences encoding each of the SH3 domains of human CIN85 [SH3-A (residues 1−58), SH3-B (residues 98−157), and SH3-C (residues 267−328)] were amplified by PCR using the cDNA of full-length CIN85 provided by SIDNET (The Signaling and Degradation Network at the Hospital for Sick Children) as a template. Each of three DNA fragments was inserted into the pET28-b vector (Novagen) enabling production of fusion proteins with His tags on their C-termini (CIN85-SH3-A-H_6, CIN85-SH3-B-H_6, and CIN85-SH3-C-H_6) when expressed in *Escherichia coli* strain BL21(DE3). To prepare ^{15}N,^{13}C-labeled or ^{15}N-labeled samples, cells were grown at 37 °C in minimal medium (M9) with [$^{13}C_6$]-D-glucose and $^{15}NH_4Cl$ or only $^{15}NH_4Cl$ as sole sources of carbon and nitrogen. The unlabeled protein was grown in LB medium. Protein expression was induced by addition of 1 mM IPTG to the cell culture, and the temperature was lowered to 25 °C during expression. The proteins were purified using Ni^{2+} chelation chromatography (HisTrap HP affinity column) followed by a gel-filtration step (Superdex 75 column). The final NMR samples contained 0.1−1 mM protein in 50 mM phosphate buffer (pH 6.4) containing 150 mM NaCl and 2 mM DTT. The F52Y mutant of the SH3-A domain was prepared using the QuikChange site-directed mutagenesis kit (Stratagene). It was expressed in unlabeled medium and purified as described above.

For ubiquitin expression, a plasmid encoding the amino acid sequence of wild-type human ubiquitin with an N-terminal His tag followed by a TEV cleavage site was used. The plasmid was transformed into *E. coli* BL21(DE3) cells. Cells were grown in minimal (M9) or rich (LB) medium depending on the desired labeling (^{15}N or unlabeled) of the protein at 37 °C until the absorbance at 600 nm reached 0.6. Protein expression was then induced by addition of 1 mM IPTG. The protein was purified using Ni^{2+}-chelation chromatography (HisTrap HP affinity column). The fusion protein was cleaved using TEV protease. Protein was then separated by a gel-filtration step (Superdex 75 column). The final NMR samples contained 0.1−1 mM protein in 50 mM phosphate buffer (pH 6.4).

The plasmids encoding G76C, I44E, and K6E ubiquitin mutants were obtained using the QuikChange site-directed mutagenesis kit (Stratagene) and the wild-type plasmid as a template. Mutants were grown and purified as for wild-type ubiquitin. In the case of G76C ubiquitin, the final buffer, however, contained no DTT. The cysteine residue of the

purified G76C ubiquitin mutant was modified with (1-oxyl-2,2,5,5-tetramethyl-3-pyrroline-3-methyl) methanesulfonate (MTSL). A 5-fold molar excess of MTSL was added to G76C ubiquitin; the reaction mixture was left overnight in the dark at 4 °C, and then the uncoupled MTSL was removed by dialysis. This yielded a paramagnetic NMR sample. To obtain the corresponding diamagnetic sample, a 29-fold molar excess of Na-L-ascorbate was added to the paramagnetic sample.

All DNA constructs were sequenced, and the purity and homogeneity of all proteins were confirmed by SDS−PAGE analysis.

NMR Spectroscopy. (i) Assignment of the CIN85 SH3-C Domain. All NMR data were acquired at 25 °C on Varian Inova 500 MHz spectrometers equipped with *z*-axis pulsed field gradient units and actively shielded triple-resonance probes. Backbone ^{1}HN, ^{13}C, and ^{15}N chemical shift assignments of the ^{15}N,^{13}C-labeled wild-type CIN85 SH3-C domain were accomplished by standard methods (*20*) using ^{1}H−^{15}N HSQC, HNCACB, and CBCA(CO)NH triple-resonance experiments. The spectra were processed with NMRPipe/NMRDraw (*21*) and analyzed with NMRView (*22*).

(ii) Chemical Shift Mapping Experiments. ^{1}H−^{15}N HSQC spectra were analyzed using the ^{1}H and ^{15}N assignments of the CIN85 SH3-C domain and ubiquitin (BMRB entry 4769). Chemical shift perturbations upon binding were measured as differences between the peak positions in the NMR spectra of free and bound protein, calculated as the root-mean-square deviations of the ^{1}H and ^{15}N resonance positions in hertz, and mapped onto the corresponding structures.

(iii) Binding Experiments. For the titration of wild-type ubiquitin with the CIN85 SH3-C domain, a 0.14 mM sample of ^{15}N-labeled ubiquitin in 50 mM phosphate buffer and 150 mM NaCl (pH 6.4) in a 90% H_2O/10% D_2O mixture with 1% DSS was used. Unlabeled CIN85 SH3-C domain was added to the NMR sample from a stock solution, which contained 14.85 mM CIN85 SH3-C domain and 0.14 mM ^{15}N-labeled ubiquitin in 50 mM phosphate buffer (pH 6.4). The CIN85 SH3-C domain was gradually added for 10 additions to a final concentration of 5.7 mM. The concentration of ubiquitin remained constant throughout the titration. K6E and I44E mutants of ubiquitin were titrated in a similar way with 11.97 and 13.2 mM stock solutions of CIN85 SH3-C, respectively. The concentrations of K6E and I44E were kept constant, 0.20 mM each, throughout the experiments.

^{1}H−^{15}N HSQC spectra were collected at each point in the titration, using 1024 complex points in the ^{1}H dimension and 64 increments in the ^{15}N dimension. Peaks were monitored for a change in chemical shift after each addition and fit according to the equation

$$[\mathrm{PL}] = {}^{1}/_{2}\{(P_\mathrm{T} + L_\mathrm{T} + K_\mathrm{D}) - [(P_\mathrm{T} + L_\mathrm{T} + K_\mathrm{D})^2 - 4P_\mathrm{T}L_\mathrm{T}]^{1/2}\}$$

where [PL] is the concentration of the complex, P_T is the total amount of protein, L_T is the total amount of ligand, and K_D is the dissociation constant.

For ubiquitin−Cbl competitive binding experiments, 0.3 mM ^{15}N-labeled ubiquitin was initially titrated with unlabeled CIN85 SH3-C domain to a final concentration of 1.0 mM (diluting ubiquitin to a concentration of 0.24 mM). Into this sample was titrated a synthetic peptide derived from human Cbl-b (residues 902−912) with the sequence PARPPK-PRPRR to a final concentration of 1.8 mM. Ubiquitin, CIN85 SH3 domain, and Cbl-derived peptide were in 50 mM phosphate buffer and 150 mM NaCl (pH 6.4) in 90% H_2O/10% D_2O. Ubiquitin chemical shift changes upon addition of the two ligands were monitored as described above for the titration of wild-type ubiquitin with the CIN85 SH3-C domain.

(iv) RDC Experiments. One-bond H−N residual dipolar couplings were measured using an IPAP experiment (*23*) on a ^{15}N-labeled 0.14 mM sample of CIN85 SH3-C domain saturated with unlabeled ubiquitin (4.6 mM) and on a ^{15}N-labeled 0.14 mM ubiquitin sample saturated with unlabeled CIN85 SH3-C domain (4.6 mM). Experiments were carried out in the absence (isotropic sample) and presence (anisotropic sample) of pf1 phage (*24*). For sample alignment, ∼8 mg of phage was added to the samples (deuterium splitting, 11.7 Hz). The magnitudes of the axial and rhombic components of the alignment tensor were obtained from a histogram of the residual dipolar coupling constants observed for saturated ubiquitin and saturated CIN85 SH3-C domain (Figure 1 of the Supporting Information), as described elsewhere (*25*). The axial and rhombic alignment tensor components thus obtained amounted to 7.74 and 0.517 Hz, respectively.

(v) PRE Experiments. PRE data were measured at 25 °C by conducting identical $^{1}H^{N}$ R_2 relaxation rate experiments on two samples. One was paramagnetic and contained 0.87 mM ^{15}N-labeled CIN85 SH3-C domain and 0.35 mM unlabeled G76C ubiquitin conjugated to MTSL. The other sample was diamagnetic and contained 10 mM Na-L-ascorbate in addition to the SH3 domain and modified G76C ubiquitin. The PRE data were calculated as a difference in $^{1}H^{N}$ R_2 rates between the paramagnetic and the diamagnetic samples. In these samples, only 30% of CIN85 was bound to ubiquitin, based on our titration data. Therefore, the measured apparent PRE data were divided by 0.3 to obtain the expected PRE data for a fully saturated CIN85 SH3-3 domain. These scaled paramagnetic rate enhancements were converted into distances as previously described by Battiste and Wagner (*26*) and used as unambiguous distance restraints in the calculations (Figure 2 of the Supporting Information).

Structural Calculations. The homology model of the CIN85 SH3-C domain was created using Modeler (*27*). A structure of the mouse CIN85 SH3-C domain (PDB entry 2DA9) was used as the template, and 10 sets of coordinates representing the model were generated (Figure 3 of the Supporting Information).

A data-based model of the complex of the CIN85 SH3-C domain with ubiquitin was generated with HADDOCK (High Ambiguity Driven protein−protein Docking) (*28*) using chemical shift perturbation data resulting from NMR titration experiments, residual dipolar couplings (*29*), and PRE-based distance restraints. Twenty residues of ubiquitin and 23 residues of the CIN85 SH3-C domain with significant chemical shift changes upon ligand binding were used for docking, and 42 and 37 RDC values for ubiquitin and CIN85 SH3-C domain, respectively, as well as 51 PRE restraints were used for the calculation of the structure of the complex. The number of RDCs values obtained is smaller than the number of residues in the SH3 domain and ubiquitin due to peak overlaps and/or broadening upon saturation and addition of phage in the sample. The ubiquitin crystal structure and

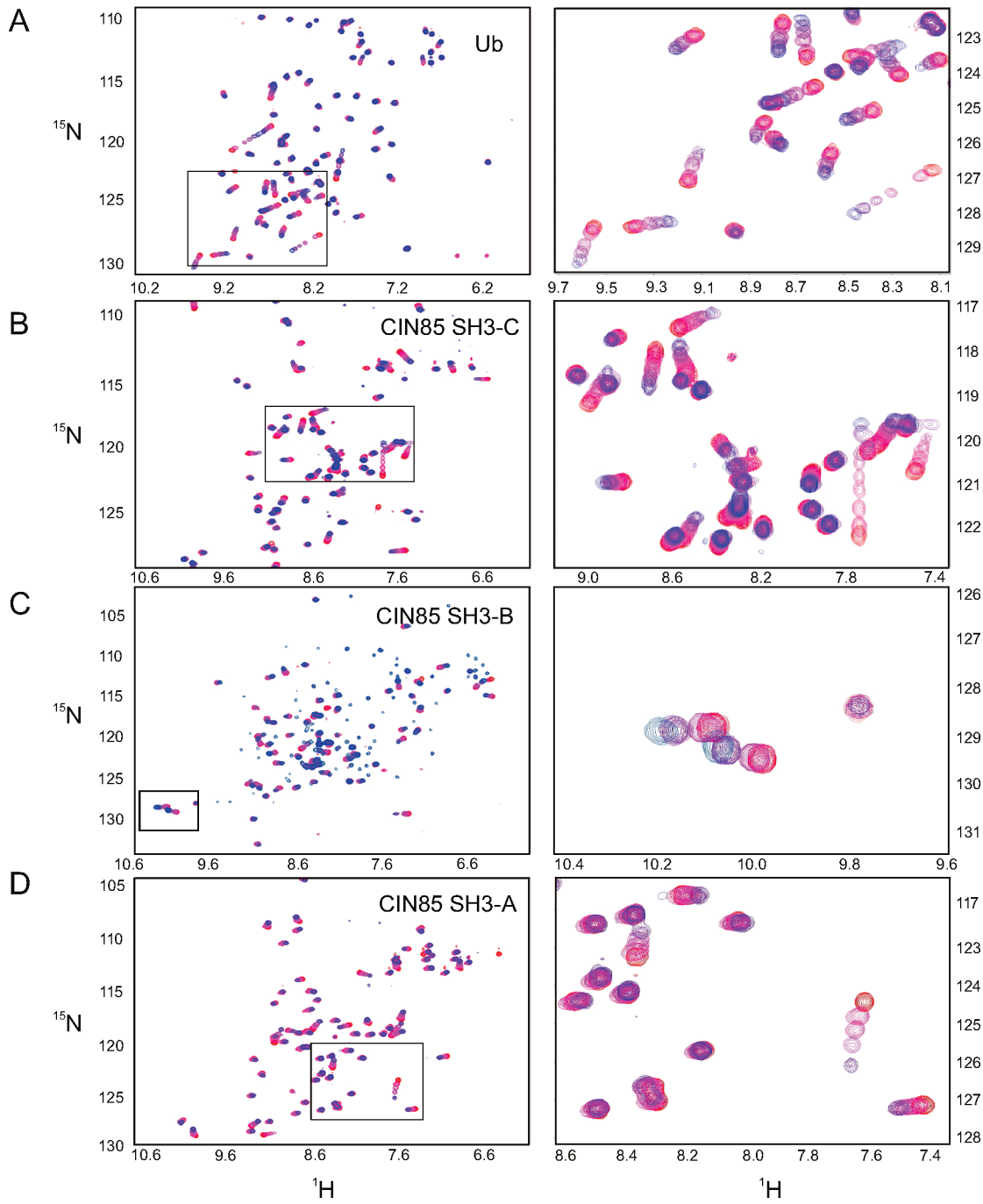

FIGURE 1: NMR titration data for binding of ubiquitin and CIN85 SH3 domains. Superposition of $^{1}H-^{15}N$ HSQC spectra of ^{15}N-labeled ubiquitin (A), CIN85 SH3-C (B), CIN85 SH3-B (C), and CIN85 SH3-A (D) domains titrated with increasing amounts of unlabeled CIN85 SH3-C domain (A) and ubiquitin (B−D). The spectra of free proteins are colored red, while the spectra of proteins at the last titration step are colored blue. Expanded regions of each overlay are shown on the right-hand side. In panel C, extra peaks emerging in the spectrum of the last titration point (blue) correspond to natural abundance ^{15}N-labeled ubiquitin.

the single lowest energy of the 10 coordinates of our homology model of the CIN85 SH3-C domain were employed. One thousand structures were calculated in the first "rigid body" docking, and then 50 lowest-energy structures were selected for the second step of refinement and analysis. The RDCs, as with all structural restraints, were used throughout the structure calculations.

Ubiquitination Assays. (i) Cell Culture and Transfection. HEK293T cells were maintained in DMEM supplemented with 10% fetal bovine serum, 100 units/mL penicillin, and 100 μg/mL streptomycin. Transient transfections were performed using the calcium phosphate precipitation method, with a total of 20 μg of DNA per 10 cm dish.

(ii) Ubiquitination Experiments. Residues F52, F151, and F322, of full-length human CIN85 in pcDNA3.1-nFlag, were mutated to Tyr (3FY) using the QuikChange mutagenesis kit (Stratagene). Cells were transfected with Flag-CIN85-WT or -3FY and His-Ub. Twenty-four hours post-transfection, the cells were serum-starved for 24 h and then treated with the proteasome inhibitor MG132 (20 μM) for 1 h before EGF stimulation (100 ng/mL for 15 min at 37 °C). Cells were lysed in ice-cold lysis buffer [50 mM Hepes (pH 7.5),

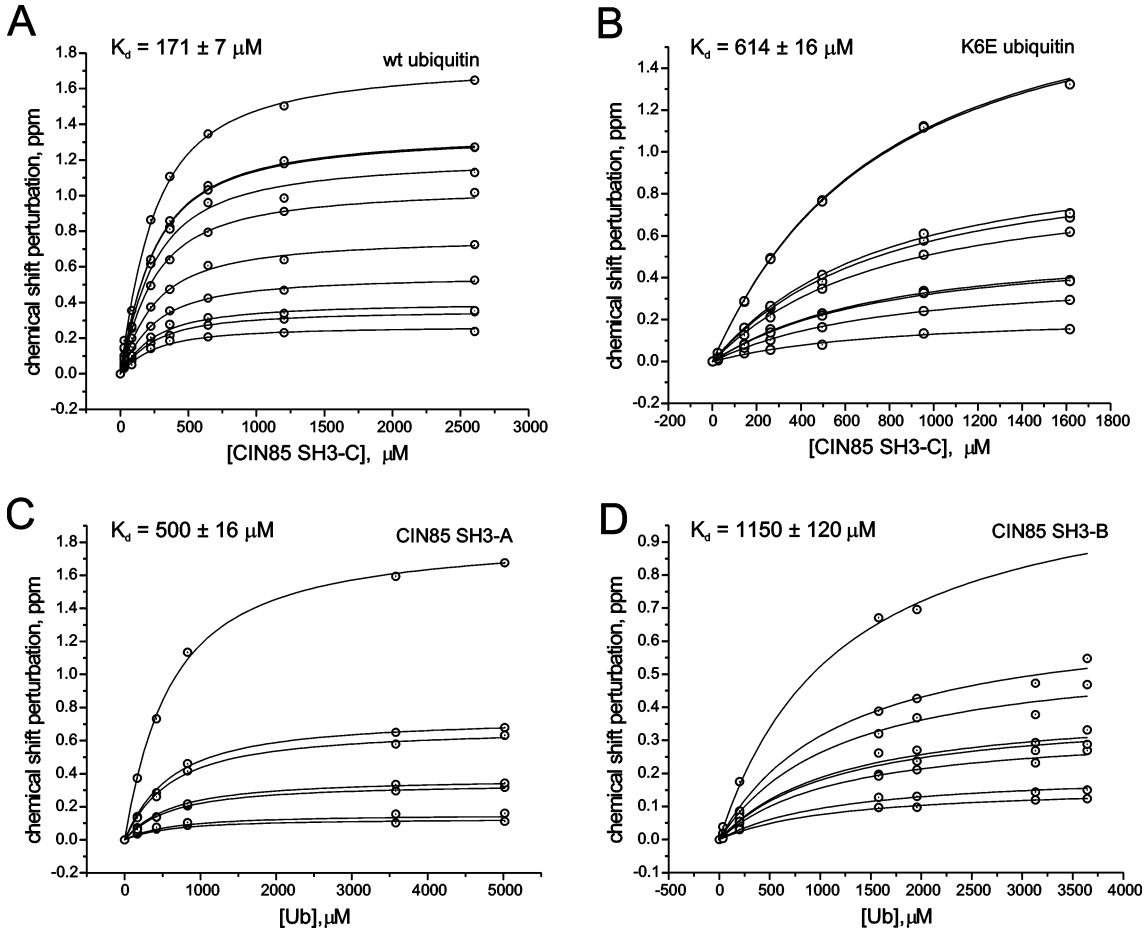

FIGURE 2: Binding curves for the ubiquitin−CIN85 SH3 domain interactions. Chemical shift perturbations upon binding to the CIN85 SH3-C domain for ten ubiquitin residues (A) and nine K6E ubiquitin mutant residues (B) plotted as a function of SH3-C domain concentration. Chemical shift perturbations for seven residues of the SH3-A (C) and eight residues of the SH3-B (D) domains of CIN85 plotted as a function of ubiquitin concentration. The K_d values were fit globally for each protein, and the fitting curves are shown.

150 mM NaCl, 1% Triton X-100, 10% glycerol, 1.5 mM $MgCl_2$, and 1 mM EGTA] supplemented with protease inhibitors (aprotinin, leupeptin, pepstatin, and PMSF), 50 μM LLnL, 0.4 mM chloroquine, 10 mM NaF, 1 mM $ZnCl_2$, and 1 mM sodium orthovanadate. Lysates with adjusted protein concentrations (Bradford assay, Bio-Rad) were denatured with 2% SDS and boiled for 5 min, and then diluted 11 times with lysis buffer to dilute SDS prior to overnight incubation with Ni-NTA agarose beads (Qiagen). Beads were washed twice with lysis buffer and twice with HNTG [20 mM Hepes (pH 7.5), 150 mM NaCl, 10% glycerol, and 0.1% Triton X-100]. Bound proteins were then eluted from beads with sample buffer, resolved by SDS−PAGE, and transferred to nitrocellulose. Membranes were probed with anti-Flag (Sigma), anti-EGFR (sc-1005, Santa Cruz), or anti-Cbl (UBI) antibodies.

Deposition of Assignments and Coordinates. ^{1}H and ^{15}N backbone and ^{13}Cα/β assignments of the CIN85 SH3-C domain and the RDC and PRE data were deposited in the BMRB (15866). The lowest-energy coordinates for the CIN85 SH3-C−ubiquitin complex were deposited in the Protein Data Bank (2K6D).

RESULTS

All Three SH3 Domains of CIN85 Bind to Ubiquitin. It has recently been reported that the third SH3 domain of the yeast endocytic protein Sla1 and the third SH3 domain of its mammalian orthologue CIN85, as well as two SH3 domains of amphiphysin, bind to the canonical hydrophobic patch on the surface of ubiquitin that serves as a binding site for all known ubiquitin binding domains (*17*). Interestingly, not all SH3 domains screened in the study bound to ubiquitin despite a high degree of sequence similarity, with the SH3-1 and SH3-2 domains of Sla1 not binding. To further investigate this intriguing interaction, we performed binding experiments with all three SH3 domains of human CIN85 using NMR titrations. We also mapped chemical shift changes on the surfaces of both interacting partners (SH3-C and ubiquitin) to identify the binding interfaces and gain structural information about the complex.

Since NMR chemical shifts are very sensitive to the local electronic environment, they can be used for mapping binding sites in protein complexes and measuring binding constants. To determine which amino acid residues of ubiquitin are involved in the interaction, a ^{15}N-labeled sample of ubiquitin was titrated with increasing amounts of unlabeled CIN85 SH3-C domain. At each point of the titration, a ^{1}H−^{15}N HSQC spectrum was recorded and chemical shift changes upon addition of ligand were measured (Figure 1A). In the same way, the binding site on the CIN85 SH3-C domain was mapped by titrating ^{15}N-labeled SH3-C domain with unlabeled ubiquitin. HSQC spectra of both the SH3-C domain and ubiquitin demonstrated selective amide proton

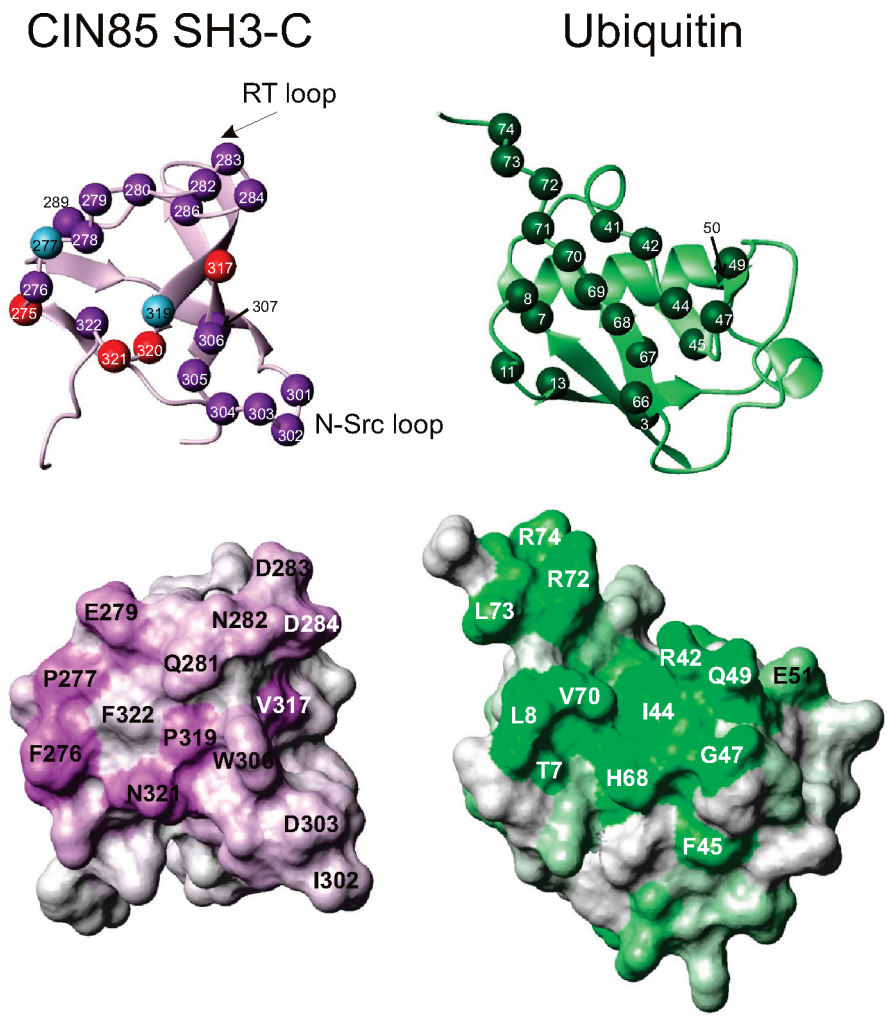

FIGURE 3: Chemical shift mapping of the CIN85 SH3-C domain−ubiquitin binding interface. Chemical shift changes in an HSQC spectrum upon binding of ubiquitin and the SH3-C domain are mapped onto the surfaces of the homology model of the CIN85 SH3-C domain and the crystal structure of ubiquitin (PDB entry 1UBQ), respectively. Chemical shift perturbations are displayed as a gradient of purple (CIN85) or green (ubiquitin) color with the largest perturbations shown in dark colors and the smallest in white. Selected residues of the binding surfaces are indicated. The ribbon diagrams of the SH3-C domain and ubiquitin in the same orientation as their surface representations are also shown above with selected residues having the greatest chemical shift perturbations upon binding labeled. Residues severely broadened upon binding are colored red, and proline residues are colored cyan.

and nitrogen chemical shift changes upon addition of binding partner, indicative of complex formation (Figure 1A,B). To test if the other two SH3 domains bind to ubiquitin, we titrated unlabeled ubiquitin into samples of ^{15}N-labeled SH3-A and SH3-B domains. As in the case of the CIN85 SH3-C domain, we observed chemical shift changes upon addition of unlabeled ubiquitin, demonstrating that both SH3 domains interact with ubiquitin (Figure 1C,D).

Binding constants (K_d values) for all SH3−ubiquitin interactions were calculated on the basis of changes in ^{1}H and ^{15}N chemical shifts of ubiquitin as a function of ligand concentration (Figure 2) (see Materials and Methods). The 10 nonoverlapping ubiquitin residues displaying the largest chemical shift changes upon binding (Ile 13, Thr 14, Leu 15, Ile 44, Gly 47, Gln 49, Leu 50, Leu 67, Val 70, and Leu 73) were used to calculate a global K_d of 171 ± 7 μM for the CIN85 SH3-C−ubiquitin interaction. Weaker binding of the SH3-A and SH3-B domains was apparent, with K_d values of 500 ± 16 and 1150 ± 120 μM, respectively, using data from nonoverlapping SH3 domain residues displaying large chemical shift changes upon ubiquitin binding. Note that the calculated K_d value for the SH3-B−ubiquitin interaction may underestimate the upper bound due to the lack of saturation of binding.

Data-Based Structural Model of the CIN85 SH3-C Domain−Ubiquitin Complex. For ubiquitin, both the tertiary structure and NMR resonance assignments are known (PDB entry 1UBQ, BMRB entry 4769), facilitating mapping of the binding site on the surface of the molecule based on chemical shift perturbations. Since there was no analogous information for human CIN85 SH3 domains available, we assigned the protein backbone resonances using standard triple-resonance NMR experiments (see Materials and Methods) on a ^{15}N,^{13}C-labeled sample of the CIN85 SH3-C domain. We then created a homology model of the isolated human CIN85 SH3-C domain using Modeler (*27*) making use of the structure of the mouse CIN85 SH3-C domain (PDB entry 2DA9), which has 93% sequence identity (Figure 3A,B of the Supporting Information).

Chemical shift changes upon ubiquitin binding were mapped onto the lowest-energy structure from the modeled human CIN85 SH3-C domain ensemble and the ubiquitin

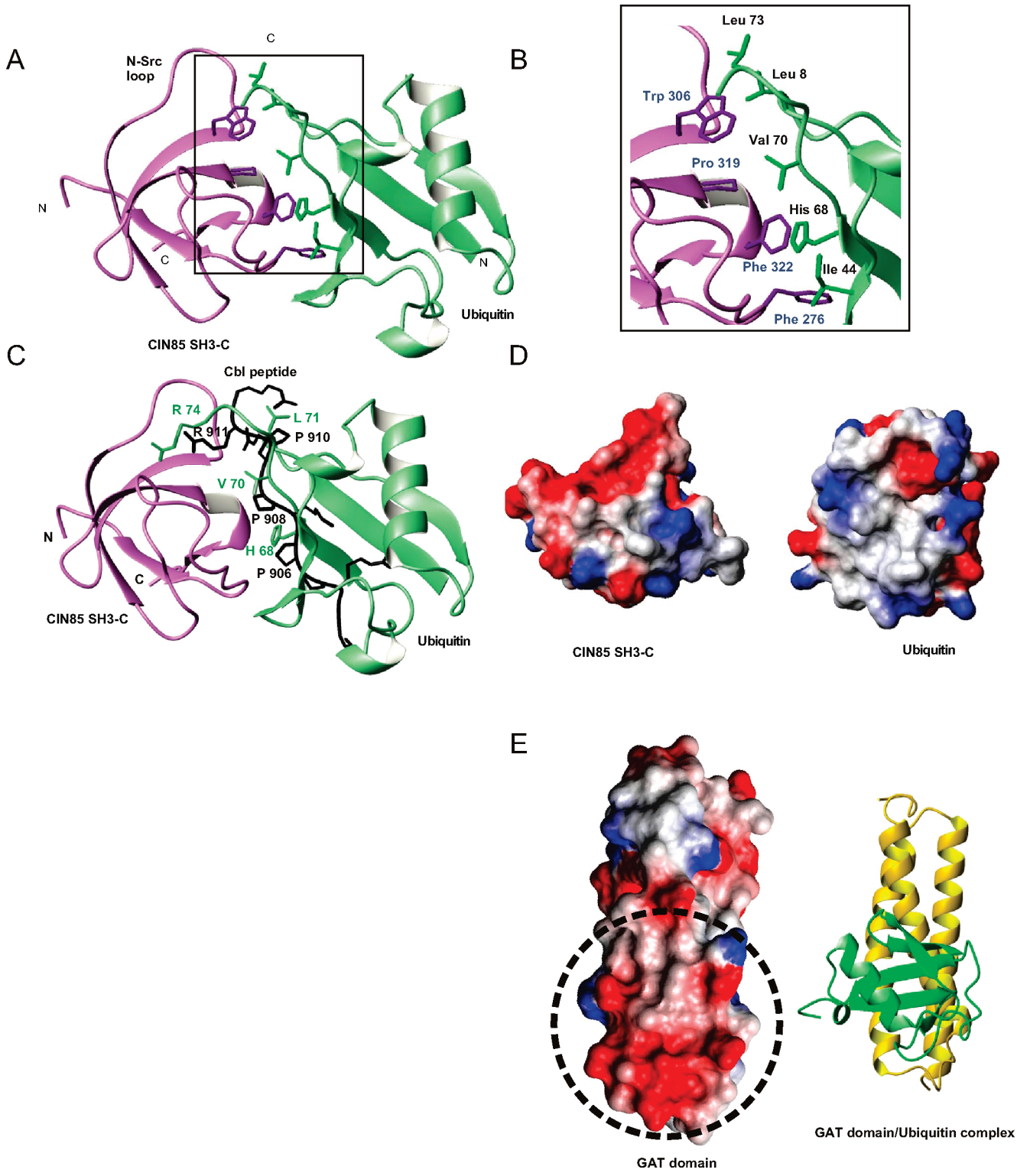

FIGURE 4: Complex between the CIN85 SH3-C domain and ubiquitin. (A) The lowest-energy structure of 50 calculated structures is shown as a ribbon diagram. The CIN85 SH3-C domain is colored purple and ubiquitin green. The interacting hydrophobic side chains in the center of the interface are represented as sticks and identified in an expanded view (B). (C) The CIN85 SH3-A domain complex with a Cbl-b peptide (PARPPKPRPRR) (PDB entry 2BZ8) is superimposed on the SH3-C domain complex with ubiquitin. The SH3-C domain is shown as a purple ribbon with ubiquitin as a green ribbon and the Cbl peptide colored black. Interacting residues of ubiquitin and the Cbl peptide are labeled in green and black, respectively. (D) Interacting surfaces of CIN85 and ubiquitin colored by their electrostatic surface potential. The CIN85 SH3-C domain structure is rotated −90° and the ubiquitin 90° along the *y*-axis with respect to their position in panels A−C to enable observation of the binding interfaces. (E) Another ubiquitin binding domain, GAT (PDB entry 1YD8), with a similarly charged ubiquitin binding site is presented for comparison. The ubiquitin binding site is outlined with a dashed circle, and a ribbon diagram of the GAT domain (yellow) in complex with ubiquitin (green) is shown at the right.

crystal structure (Figure 3). The largest perturbations which correspond to the binding sites are localized to discrete surfaces on the two proteins. The ubiquitin binding site involves Ile 44 and residues around it, including Thr 7, Leu 8, Ile 13, Arg 42, Phe 45, Gly 47, Gln 49, Phe 50, Leu 67, His 68, Leu 69, and Val 70, and corresponds to the region

Table 1: Structural Statistics for the CIN85 SH3-C Domain−Ubiquitin Complex

Deviations from Experimental Restraints (RDC *R*-Factors)[a]	
CIN85	0.18 ± 0.01
ubiquitin	0.12 ± 0.01
Structural Precision [rmsd (Å)[b]]	
CIN85 with ubiquitin	
backbone	1.9 ± 0.6 (1.4 ± 0.6)
heavy	2.2 ± 0.6 (1.7 ± 0.5)
CIN85	
backbone	0.7 ± 0.2
heavy	1.0 ± 0.2
ubiquitin	
backbone	1.8 ± 0.5 (0.7 ± 0.2)
heavy	2.1 ± 0.5 (1.1 ± 0.3)
Deviations from Standard Covalent Geometry	
bonds (Å)	0.009 ± 0.000
angles (deg)	1.0 ± 0.0
dihedrals (deg)	22.6 ± 0.5
impropers (deg)	1.63 ± 0.03
Percentage of Residues in Different Regions of the Ramachandran Diagram	
most favored regions	90.2
additional allowed regions	8.5
generously allowed regions	1.2
disallowed regions	0.1

[a] The residual dipolar coupling (RDC) *R*-factor is defined as the ratio of the rms deviation between observed and calculated values to the expected rms deviation if the vectors were randomly oriented. The latter is given by $[2D_a^2(4 + 3R^2)/5]^{1/2}$, where D_a is a magnitude of the axial component of the alignment tensor and *R* the rhombicity (*38*). [b] The rms deviations are given for all residues and, in parentheses, without considering the four C-terminal residues of ubiquitin, which are poorly defined.

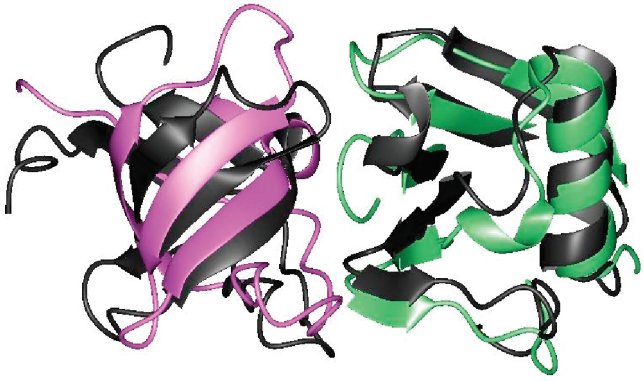

FIGURE 5: Comparison of the complexes of the CIN85 SH3-C and Sla1 SH3-3 domains with ubiquitin. Superposition of the two complexes, with the Sla1 SH3-3 domain−ubiquitin complex colored black, the CIN85 SH3-C domain colored purple, and ubiquitin colored green.

recognized by most ubiquitin binding domains (*18*). The CIN85 SH3-C domain interface primarily includes the RT- and N-Src loops and three-residue helical turn (residues 320−322) with the Phe 322 and Trp 306 side chains in the center of the binding surface (see Figure 3). Other residues on this interface include Phe 376, Glu 379, Gln 381, Asn 382, Asp 383, and Asp 384. This region corresponds to the classical SH3 domain site responsible for binding to PPII helical, proline-rich targets, as shown in Figure 4C with the structure of the CIN85 SH3-A domain bound to a Cbl peptide (PDB entry 2BZ8) superimposed on our structure of the SH3-C domain bound to ubiquitin. The observed overlap between the surfaces for binding canonical proline-rich peptides and ubiquitin is in close agreement with mutational data defining the ubiquitin binding site on the Sla1 SH3 domain and the Sla1 SH3-3 domain−ubiquitin complex (*17*).

A data-based structural model of the complex between the CIN85 SH3-C domain and ubiquitin was calculated using HADDOCK (*28*), which docks two molecules of known structure based on various experimental data, including NMR chemical shift perturbations. The crystal structure of free ubiquitin and the homology model of the SH3-C domain together with the chemical shift perturbations were used to model the structure of the ubiquitin−CIN85 SH3-C domain complex. Additional experimental structural data for the complex were obtained by measuring paramagnetic relaxation enhancement (PRE) and H−N residual dipolar coupling (RDC) values (*29, 30*) (Figure 1 of the Supporting Information). PREs were introduced using the paramagnetic label, MTSL, attached to the C-terminus of unlabeled ubiquitin in complex with the ^{15}N-labeled CIN85 SH3-C domain (Figure 2 of the Supporting Information). Measured PRE values provide restraints on long-range intermolecular distances, while H−N RDCs supply information about the relative orientation of HN bond vectors in the molecule. The RDC and PRE data comprised experimental structural information about the two proteins in their bound states as well as the orientation of the two proteins with respect to each other.

In this regard, RDCs have been increasingly utilized as a rapid approach to gaining structural restraints (*31–34*). Several applications have utilized RDCs as a primary source of restraints for de novo structure determination. The high-resolution structure of cytochrome *c′* was determined using RDC restraints and paramagnetic restraints (*33*); the global fold of a three-helix bundle has been determined using RDC restraints supplemented with a limited number of NOE distance restraints (*32*), and for the small protein ubiquitin, a high-resolution structure has been determined using only RDC restraints by two independent methods (*31, 34*). While the use of only one set of RDCs may not be enough for de novo structure determination, multiple sets of RDC restraints or RDC restraints supplemented with an alternate source of information, such as PRE restraints or statistical ab initio protein structure prediction methods (*35*), have proven to be sufficient for structure determination. Here we supplement chemical shift mapping data defining the interface with PRE and RDC restraints to determine a structural model of the SH3-C domain in complex with ubiquitin.

Of 50 calculated structures, 42 were in the same orientation. Structural statistics for this ensemble of 42 complexes are presented in Table 1, showing good agreement with experimental restraints. Details of RDC and PRE restraints are also provided in Figures 1 and 2 of the Supporting Information. The lowest-energy coordinates of the complex are presented in Figure 4. As expected on the basis of the chemical shift changes mapped and the Sla1 complex, the two proteins utilize their classic binding sites to form the complex. The calculated model is similar to the Sla1 SH3-3 domain−ubiquitin structure with a backbone rmsd of 3.8 Å for the lowest-energy coordinates and 4.1 ± 0.3 Å for the 10 lowest-energy coordinates (Figure 5). A somewhat high rmsd between the two complexes arises mainly from the differences between the individual proteins rather than the protein−ligand orientation. For example, the rmsd between the SH3 domains is 2.7 Å (2.5 ± 0.1 Å) and

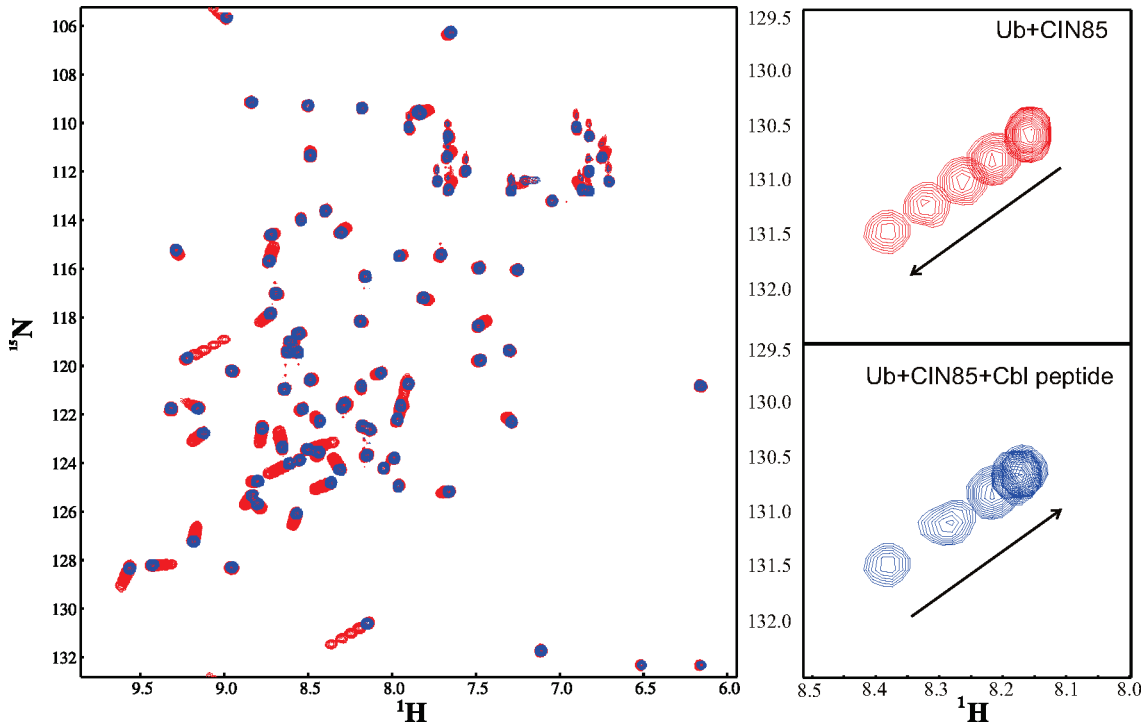

FIGURE 6: Competition between ubiquitin and Cbl peptide for CIN85 SH3-C domain binding. ^{15}N-labeled ubiquitin (0.2 mM) was titrated with the unlabeled CIN85 SH3-C domain (0, 0.2, 0.3, 0.5, and 1.0 mM) and then at the highest concentration of the SH3 domain additionally titrated with unlabeled Cbl peptide (0, 0.2, 0.5, 0.9, and 1.9 mM). In the left panel, ^{1}H−^{15}N HSQC spectra of ubiquitin for all the CIN85 SH3-C titration points (red) and the final Cbl peptide titration point (blue) are superimposed. In the right panel, the chemical shift changes upon addition of the SH3 domain to ubiquitin (top, red) and the subsequent addition of Cbl peptide (bottom, blue) are shown for a selected peak, with arrows indicating the direction of peak movement upon addition of increasing amounts of the ligands.

between the two complexed ubiquitins is 2.2 Å (2.3 ± 0.1 Å). These differences may result from a sequence identity of only 34% between the yeast Sla1 SH3-3 domain and the human CIN85 SH3-C domain.

The interface consists of a core of hydrophobic residues in the center of the binding surface with charged/polar residues flanking the interface (Figure 4A,B,D). Phe 322 and Trp 306 in the SH3-C domain form central hydrophobic interactions with His 68 and Ile 44, and Ile 8 and Leu 73, respectively, of ubiquitin. Other important interactions include interactions of CIN85 Phe 276 with His 68 and Ile 44 of ubiquitin and Pro 319 with Val 70 of ubiquitin. To test the importance of the observed interactions within the structure of the complex, we introduced two mutations into the ubiquitin binding site, I44E and K6E, and repeated the NMR binding experiments. The I44E mutant lost the ability to bind to the SH3-C domain (data not shown), while the K6E mutant bound significantly more weakly than the wild type, with a K_d of 614 ± 16 μM (Figure 2), again with the upper bound potentially underestimated due to a lack of saturation of binding.

Ubiquitin Competes with Cbl for CIN85 Binding. To show that ubiquitin and Cbl compete for the same binding site on the CIN85 SH3 domains, we recorded HSQC spectra of ^{15}N-labeled ubiquitin while titrating with increasing amounts of unlabeled CIN85 SH3-C domain and monitored the chemical shift changes reflecting the binding of ubiquitin to the SH3 domain (Figure 6). To this CIN85−ubiquitin complex was then gradually added a Cbl-b derived proline-rich peptide (PARPPKPRPRR), which resulted in the movement of the chemical shifts of ubiquitin back to those of the free state. The results indicate the release of ubiquitin from the complex and its substitution by Cbl peptide and confirm that ubiquitin and Cbl compete for binding to the CIN85 SH3 domain.

Effect of the CIN85−Ubiquitin Interaction on Ubiquitination of CIN85. Mutation of Phe in the hydrophobic groove of the Sla1 SH3-3 domain to Tyr was shown to prevent ubiquitin binding but not affect binding to the PxxxPR motif of Cbl (*17*). Using NMR, we also showed that the F52Y mutation of the CIN85 SH3-A domain prevents its binding to ubiquitin (Figure 4 of the Supporting Information). On the basis of these data and our structural studies, we designed a CIN85 construct in which all three SH3 domains had such F → Y mutations. Since in the mammalian CIN85 all three SH3 domains contain a Phe at that position [unlike Sla1, in which only the third SH3 domain has an equivalent Phe (*17*)], we mutated all three phenylalanines (F52Y, F151Y, and F322Y) to produce a CIN85 protein unable to bind ubiquitin effectively but able to recognize PPII motifs, as found in Cbl and other targets. We refer to this mutant as 3FY hereafter.

HEK293T cells, transfected with wild-type (WT) Flag-CIN85 or Flag-CIN85-3FY and histidine-tagged ubiquitin (His-Ub), were stimulated with EGF to induce Cbl-mediated CIN85 ubiquitination. Ubiquitinated CIN85 was precipitated from cell lysates using Ni-NTA agarose beads and detected by immunoblotting with Flag antibodies. Upon EGF stimulation, the amount of ubiquitinated Flag-CIN85-WT dramatically increased, consistent with previous reports (*2*). However, in the case of the ubiquitin binding impaired mutant Flag-CIN85-3FY, CIN85 became ubiquitinated even in the absence of EGF stimulation (Figure 7A). Importantly, the levels of endogenous Cbl expression are equivalent in the absence and presence of EGF (Figure 7C), confirming

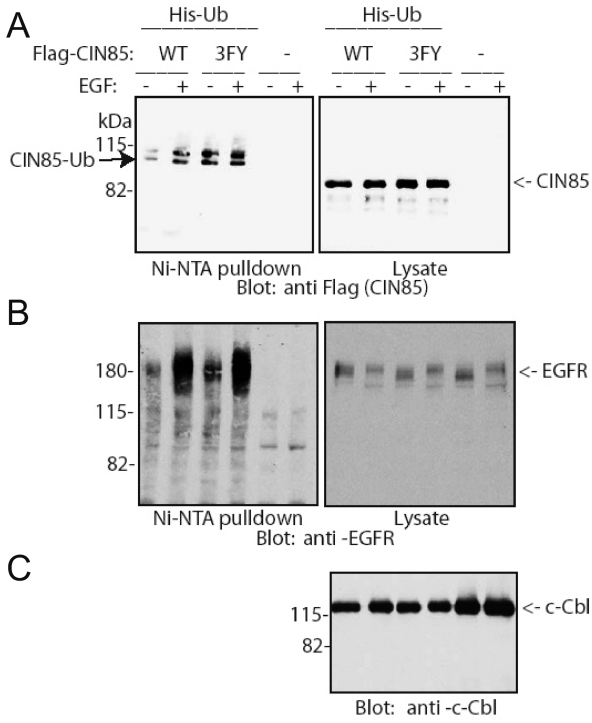

FIGURE 7: Ubiquitination of wild-type CIN85 and the 3FY (ubiquitin binding impaired) mutant CIN85. (A) HEK293T cells overexpressing His-tagged ubiquitin and Flag-tagged CIN85 or Flag-tagged 3FY mutant were stimulated with EGF. Ubiquitinated proteins in total cell lysate were precipitated using Ni-NTA pulldown and were analyzed for the presence of ubiquitinated CIN85 (WT or 3FY mutant) before and after EGF stimulation by blotting with anti-Flag antibodies (left panel). Levels of CIN85 WT and 3FY mutant expression in the total cell lysate are shown in the right panel. (B) HEK293T cells overexpressing His-tagged ubiquitin and Flag-tagged CIN85 WT or 3FY mutant were stimulated with EGF. Ubiquitinated proteins in total cell lysate were precipitated using Ni-NTA pulldown and were analyzed for the presence of ubiquitinated endogenous EGFR before and after EGF stimulation by blotting with anti-EGFR antibodies (left panel). Levels of EGFR expression in the total cell lysate are shown in the right panel. (C) Levels of endogenous Cbl expression in the total cell lysate.

that the effects are due to differences in CIN85 ubiquitin binding. Unlike other ubiquitin binding domain-containing proteins, we found that ubiquitin binding was not required for CIN85 monoubiquitination. While previous reports have suggested that CIN85 is primarily monoubiquitinated (*2*), the pattern of ubiquitination observed here is indicative of mono- and diubiquitination of CIN85.

We also examined whether EGFR ubiquitination is affected by overexpression of Flag-CIN85-WT or -3FY. Using a Ni-NTA agarose pulldown and immunoblotting for EGFR, we observed EGFR ubiquitination upon EGF stimulation when either Flag-CIN85-WT or -3FY was overexpressed. Notably, cells expressing Flag-CIN85-3FY display EGFR ubiquitination even in the absence of EGF stimulation, albeit at significantly lower levels (Figure 7B). Similar experiments with the ubiquitin I44E mutant were not undertaken since the necessity of this site for many ubiquitin interactions in the cell and in this pathway would likely preclude a reasonable interpretation of results. Taken together, our data suggest that ubiquitin binding by CIN85 negatively regulates CIN85 ubiquitination.

DISCUSSION

Structural Analysis of the CIN85 SH3-C Domain−Ubiquitin Interaction. Work by Stamenova et al. (*17*) presented evidence of an interaction between ubiquitin and several SH3 domains, including the SH3-3 of Sla1, SH3-C of CIN85, and the SH3 domains of amphiphysins I and II. This study also demonstrated that the SH3 domain−ubiquitin interaction is not universal, with the two N-terminal SH3 domains of Sla1, the N-terminal SH3 domain of Grb2, and the endophilin B1 SH3 domain not interacting with ubiquitin despite their high degree of sequence similarity. Mutational analysis of the SH3-3 domain of Sla1 identified the hydrophobic groove of the SH3 domain as the ubiquitin binding site. Comparison of Sla1 SH3-3 and CIN85 SH3-C domains with nonbinding Sla1 and Grb2 SH3 domains identified only one surface residue unique to SH3 domains binding ubiquitin. This residue is Phe (position 409 in full-length Sla1) in the SH3-3 domain and Tyr in both SH3-1 (position 64) and SH3-2 (position 126) domains. Alignment of SH3 domain sequences revealed that those domains containing Tyr in the position corresponding to Phe 409 of Sla1 did not bind to ubiquitin, while sequences with Phe did. Moreover, mutating Phe 409 to Tyr in the SH3-3 domain prevented ubiquitin binding (*17*). Consistently, in this work, we have shown that the F52Y mutant of the CIN85 SH3-A domain abolishes the interaction with ubiquitin (Figure 4 of the Supporting Information), confirming that a Phe residue in this position is critical for ubiquitin binding by SH3 domains.

In our current study of the mammalian orthologue of Sla1, CIN85, we showed that all three SH3 domains interact with ubiquitin with the SH3-C domain binding most strongly and SH3-B binding most weakly. The structure of the complex of the CIN85 SH3-C domain with ubiquitin rationalizes the importance of Phe 322 (Phe 409 in the Sla1 SH3-3 domain) for complex formation. Analysis of the binding interface reveals that the Phe 322 side chain, similar to Phe 409 of Sla1, is making extensive contacts with Ile 44 of ubiquitin (Figure 4). The introduction of the polar OH group of Tyr into this hydrophobic environment likely leads to electrostatic and steric repulsion between the two proteins, as we observed in a model built with the Tyr substitution (data not shown). Ile 44 of ubiquitin is the residue known to be in the center of interaction interfaces with most ubiquitin binding domains (*18*). Mutation of Ile 44 has been shown to prevent binding to ubiquitin binding domains. Consistently, the I44E mutation prevents binding to the SH3-C domain of CIN85 in our study.

Unlike the Sla1 SH3 domains, all three SH3 domains of CIN85 have a Phe at the position corresponding to Phe 322 of the SH3-C domain, and all bind to ubiquitin. This suggests that full-length CIN85, with three ubiquitin-binding sites, may interact more efficiently with ubiquitin. Another crucial interaction is the one between Trp 306 of the SH3-C domain and Leu 8 of ubiquitin. Trp 306 is also the central residue in the binding of SH3 domains to their proline-rich targets, and mutation of this residue affects binding to both the canonical PPII targets and ubiquitin (*17, 36*). As seen in Figures 4C and 6, the SH3-C domain uses the same binding surface for ubiquitin binding as it does for the binding to these PPII targets. Moreover, the central part of the interacting C-terminus of ubiquitin (residues 68−70) mimics a three-residue PPII turn. NMR spectra monitoring titrations of

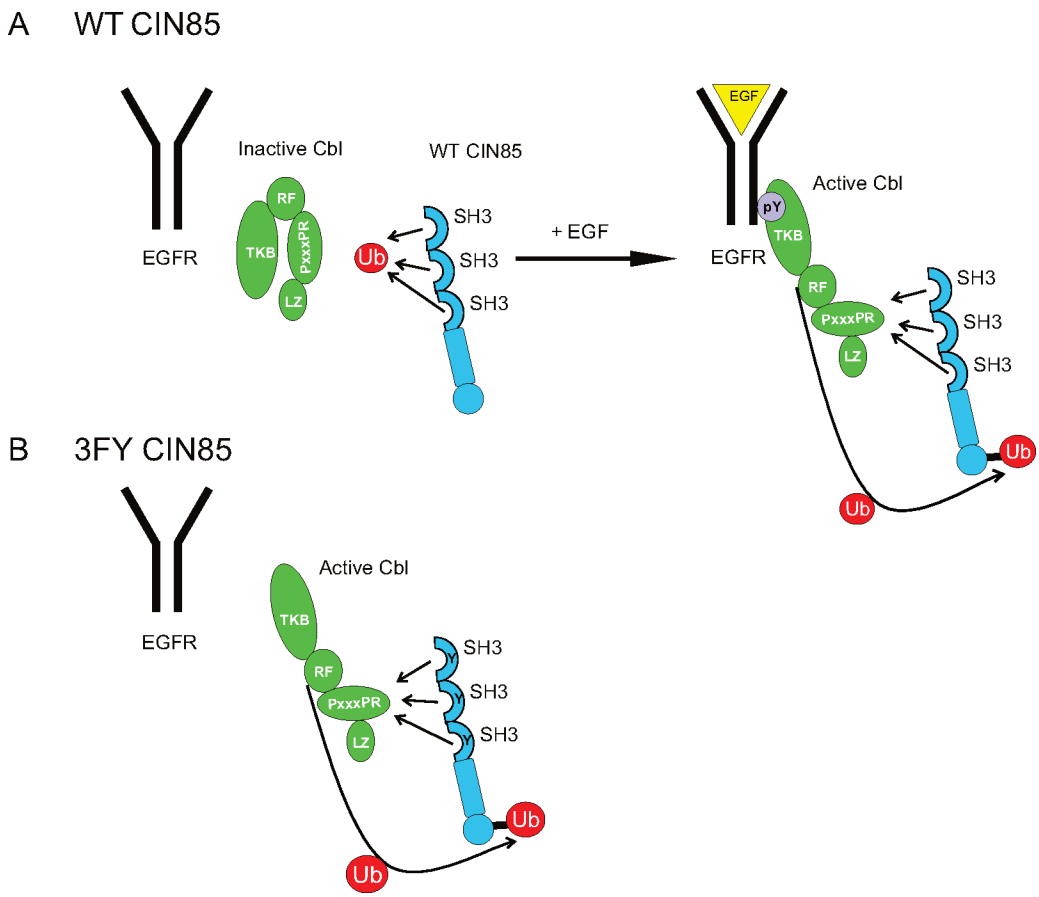

FIGURE 8: Model for the role of ubiquitin binding in the ubiquitination of CIN85. (A) In the absence of EGF, CIN85 is bound to ubiquitin and Cbl is in its inactive conformation. Following EGF stimulation, the EGF receptor (EGFR) is phosphorylated and Cbl binds to phospho-EGFR with its TKB domain, exposing or stabilizing the Cbl PPII target sequence recognized by SH3 domains of CIN85. SH3 domains of CIN85, having higher affinity for the Cbl PxxxPR motif compared to that of ubiquitin, preferentially bind Cbl, and CIN85 is ubiquitinated. (B) The 3FY mutant of CIN85 that is impaired in its ability to bind ubiquitin binds to Cbl even in the absence of EGF and stabilizes Cbl in its active conformation, leading to constitutive ubiquitination of CIN85.

SH3-A and SH3-B domains with ubiquitin show that they bind to ubiquitin via the same hydrophobic groove as the SH3-C domain since the NMR resonances of the side chains of two Trp residues located in the PPII binding site of SH3 domains are among those experiencing significant chemical shift perturbations (Figure 1C,D).

Ubiquitin binding proteins generally have small, independently folding ubiquitin binding domains or "motifs" that can interact directly with monoubiquitin and/or polyubiquitin chains. At least 10 different types of structurally diverse ubiquitin binding domains have been identified (*17, 18*). Comparing the structures of known ubiquitin binding domains with the CIN85 SH3-C domain reveals that, despite their topological diversity, the ubiquitin binding sites in all these domains have similar electrostatic surfaces. All of them contain a central hydrophobic patch flanked with mostly negatively charged residues very similar to the ubiquitin binding surface of the CIN85 SH3-C domain, as illustrated for the GAT domain of bovine ADP-ribosylation factor binding protein GGA3 (Figure 4D,E). Thus, the similarity of the electrostatic surface of the CIN85 SH3-C domain containing a central hydrophobic region surrounded by negative potential provides an explanation for the unusual binding to ubiquitin. Note that the degree of sequence identity among the three CIN85 SH3 domains is high (52% identical and 69% similar between SH3-A and -C domains, 47% identical and 68% similar between SH3-B and -C domains, and 42% identical and 62% similar between SH3-A and -B domains) with similar electrostatic surfaces, and overall highly similar ubiquitin interaction surfaces, expected for each (Figure 3C,D of the Supporting Information).

The CIN85 SH3-C Domain−Ubiquitin Interaction Plays a Role in EGF-Dependent Ubiquitination. Many ubiquitin receptors are themselves ubiquitinated, in a process termed coupled monoubiquitination, for which ubiquitin binding is essential. In some cases, monoubiquitination functions to prevent binding of these proteins to their ubiquitinated targets through formation of intramolecular interactions between ubiquitin and their ubiquitin binding domains (*37*). In the case of CIN85, however, ubiquitin binding is not required for its Cbl-mediated ubiquitination since we observed similar levels of ubiquitinated CIN85-WT and -3FY after EGF stimulation. Interestingly, the inability of the 3FY mutant to bind ubiquitin results in its constitutive ubiquitination (Figure 7), suggesting that ubiquitin binding inhibits CIN85 ubiquitination in the absence of stimulation.

There is evidence to suggest that EGF-induced Cbl binding to phospho-EGFR followed by phosphorylation of Cbl causes a conformational change in its C-terminus, which may expose or stabilize the CIN85 SH3 domain binding site, enhancing the CIN85−Cbl interaction (*3*). This is supported by data showing that the Cbl-b mutant lacking its N-terminal TKB domain (i.e., unable to bind EGFR but capable of CIN85 binding) strongly promotes ubiquitination of CIN85 even in

the absence of EGF stimulation (*2*), suggestive of an intramolecular interaction involving the TKB domain of Cbl that masks the CIN85 binding site in the absence of EGF. The intramolecular interaction would be disrupted when Cbl binds to phosphorylated EGFR upon EGF stimulation, leading to a conformational change and subsequent exposure of the PxxxPR motif.

Since ubiquitin shares the same binding site as classical targets of SH3 domains of CIN85, ubiquitin can compete with them for binding to CIN85 and thus affect the interaction of CIN85 with Cbl. Indeed, we clearly demonstrate the competition between ubiquitin and a Cbl-derived PxxxPR peptide for CIN85 SH3-C domain binding (Figure 6). This competition, together with the two conformational states of the Cbl PxxxPR motif, helps explain our observation that ubiquitin binding by CIN85 is required for its ubiquitination to be EGF-dependent. We propose a simplified model in which an equilibrium exists between CIN85 SH3 domains binding to ubiquitin and to Cbl. Shifts in this equilibrium induced by changes in accessibility to the PxxxPR sequence in Cbl act as a switch for Cbl activation and subsequent CIN85 ubiquitination (Figure 8). In the absence of EGF stimulation, CIN85 might preferentially bind to ubiquitin via its SH3 domains, while Cbl is in its "inactive" conformation. EGF stimulation leads to EGF receptor phosphorylation, creating a binding site for the TKB domain of Cbl. This is followed by phosphorylation of Cbl and generation of the "active" conformation with an exposed or stabilized PPII sequence able to be recognized by the SH3 domains of CIN85. The SH3 domains of CIN85, having an affinity for the exposed PxxxPR motif of Cbl 2 orders of magnitude higher than that of ubiquitin (*17*), preferentially bind to Cbl, and CIN85 is ubiquitinated by Cbl. If the interaction of CIN85 with ubiquitin is disrupted, as in the case of the 3FY mutant, the equilibrium is shifted toward Cbl binding, leading to CIN85 ubiquitination even in the absence of EGF stimulation. Although Cbl does not bind the receptor in the absence of EGF, the presence of "activated" Cbl in the proximity of the receptor leads to low levels of EGFR ubiquitination (Figure 7B).

It is important to consider the state of ubiquitin that binds to the CIN85 SH3 domains. The ubiquitin molecule may be conjugated to a protein that is ubiquitinated rather than being free ubiquitin. If the ubiquitinated protein is localized within a larger macromolecular complex with CIN85, this would increase the local concentration and apparent affinity for the SH3 domains. Thus, the binding affinities of the CIN85 SH3 domains for Cbl and ubiquitin in the cell may not differ by as much as the 2 orders of magnitude observed for an isolated SH3 domain binding to an isolated proline-rich peptide and free ubiquitin. The association of CIN85 with Cbl and ubiquitin is also likely to be affected by other local interactions within full-length Cbl, CIN85, and the targeted ubiquitinated protein(s), including multiple SH3 domains binding to multiple proline-rich sequences within Cbl and within CIN85 itself, as well as binding of ubiquitin to the C-terminal ubiquitin-binding domain within Cbl. Stable binding of CIN85 at the Cbl proline-rich sequence site may not even be required, as the conformational change leading to Cbl activation could be effected by only transient CIN85 SH3 domain association and then locked in by binding of the ligase substrates. There may also be involvement of other ubiquitin ligases such as Nedd4 in the ubiquitination of CIN85 (*2*). Thus, the model proposed above is likely a simplified version. We can conclude, however, that the CIN85−ubiquitin interaction has a significant effect on cell signaling and inhibits the ubiquitination of CIN85 in the absence of EGF stimulation.

The current structural data for the CIN85 SH3 domain complex with ubiquitin enhance our understanding of the in vivo CIN85 ubiquitination data, suggesting an important role of competition for protein interaction sites in the process of clathrin-mediated receptor endocytosis. The presence of such dynamic equilibria in the regulation of many biochemical processes has been seen previously. Further studies of the significance of ubiquitin competition in these equilibria will likely provide many insights into biological function given the preponderance of ubiquitin and of domains capable of binding ubiquitin.

ACKNOWLEDGMENT

We thank Drs. L. E. Kay, D. M. Korzhnev, and R. Muhandiram for their valuable help with NMR experiments.

SUPPORTING INFORMATION AVAILABLE

Four supplementary figures providing sequence, structural, and NMR data for the CIN85 SH3 domains and NMR titration data demonstrating the inability of the F52Y mutant of the SH3-A domain of CIN85 to bind ubiquitin. This material is available free of charge via the Internet at http://pubs.acs.org.

REFERENCES

1. Levkowitz, G., Waterman, H., Zamir, E., Kam, Z., Oved, S., Langdon, W. Y., Beguinot, L., Geiger, B., and Yarden, Y. (1998) c-Cbl/Sli-1 regulates endocytic sorting and ubiquitination of the epidermal growth factor receptor. *Genes Dev. 12*, 3663–3674.
2. Haglund, K., Shimokawa, N., Szymkiewicz, I., and Dikic, I. (2002) Cbl-directed monoubiquitination of CIN85 is involved in regulation of ligand-induced degradation of EGF receptors. *Proc. Natl. Acad. Sci. U.S.A. 99*, 12191–12196.
3. Soubeyran, P., Kowanetz, K., Szymkiewicz, I., Langdon, W. Y., and Dikic, I. (2002) Cbl-CIN85-endophilin complex mediates ligand-induced downregulation of EGF receptors. *Nature 416*, 183–187.
4. Thien, C. B. F., and Langdon, W. Y. (2001) Cbl: Many adaptations to regulate protein tyrosine kinases. *Nat. Rev. Mol. Cell Biol. 2*, 294–305.
5. Take, H., Watanabe, S., Takeda, K., Yu, Z. X., Iwata, N., and Kajigaya, S. (2000) Cloning and characterization of a novel adaptor protein, CIN85, that interacts with c-Cbl. *Biochem. Biophys. Res. Commun. 268*, 321–328.
6. Kuriyan, J., and Cowburn, D. (1997) Modular peptide recognition domains in eukaryotic signaling. *Annu. Rev. Biophys. Biomol. Struct. 26*, 259–288.
7. Dikic, I., Szymkiewicz, I., and Soubeyran, P. (2003) Cbl signaling networks in the regulation of cell function. *Cell. Mol. Life Sci. 60*, 1805–1827.
8. Jozic, D., Cardenes, N., Deribe, Y. L., Moncalian, G., Hoeller, D., Groemping, Y., Dikic, I., Rittinger, K., and Bravo, J. (2005) Cbl promotes clustering of endocytic adaptor proteins. *Nat. Struct. Mol. Biol. 12*, 972–979.
9. Kowanetz, K., Husnjak, K., Holler, D., Kowanetz, M., Soubeyran, P., Hirsch, D., Schmidt, M. H. H., Pavelic, K., De Camilli, P., Randazzo, P. A., and Dikic, I. (2004) CIN85 associates with multiple effectors controlling intracellular trafficking of epidermal growth factor receptors. *Mol. Biol. Cell 15*, 3155–3166.
10. Dikic, I. (2002) CIN85/CMS family of adaptor molecules. *FEBS Lett. 529*, 110–115.
11. Gout, I., Middleton, G., Adu, J., Ninkina, N. N., Drobot, L. B., Filonenko, V., Matsuka, G., Davies, A. M., Waterfield, M., and

Buchman, V. L. (2000) Negative regulation of PI 3-kinase by Ruk, a novel adaptor protein. *EMBO J. 19*, 4015–4025.
12. Lynch, D. K., Winata, S. C., Lyons, R. J., Hughes, W. E., Lehrbach, G. M., Wasinger, V., Corthals, G., Cordwell, S., and Daly, R. J. (2003) A cortactin-CD2-associated protein (CD2AP) complex provides a novel link between epidermal growth factor receptor endocytosis and the actin cytoskeleton. *J. Biol. Chem. 278*, 21805–21813.
13. Tibaldi, E. V., and Reinherz, E. L. (2003) CD2BP3, CIN85 and the structurally related adaptor protein CMS bind to the same CD2 cytoplasmic segment, but elicit divergent functional activities. *Int. Immunol. 15*, 313–329.
14. Boggon, T. J., and Eck, M. J. (2004) Structure and regulation of Src family kinases. *Oncogene 23*, 7918–7927.
15. Watanabe, S., Take, H., Takeda, K., Yu, Z. X., Iwata, N., and Kajigaya, S. (2000) Characterization of the CIN85 adaptor protein and identification of components involved in CIN85 complexes. *Biochem. Biophys. Res. Commun. 278*, 167–174.
16. Borinstein, S. C., Hyatt, M. A., Sykes, V. W., Straub, R. E., Lipkowitz, S., Boulter, J., and Bogler, O. (2000) SETA is a multifunctional adapter protein with three SH3 domains that binds Grb2, Cbl, and the novel SB1 proteins. *Cell. Signalling 12*, 769–779.
17. Stamenova, S. D., French, M. E., He, Y., Francis, S. A., Kramer, Z. B., and Hicke, L. (2007) Ubiquitin binds to and regulates a subset of SH3 domains. *Mol. Cell 25*, 273–284.
18. Hicke, L., Schubert, H. L., and Hill, C. P. (2005) Ubiquitin-binding domains. *Nat. Rev. Mol. Cell Biol. 6*, 610–621.
19. He, Y., Hicke, L., and Radhakrishnan, I. (2007) Structural basis for ubiquitin recognition by SH3 domains. *J. Mol. Biol. 373*, 190–196.
20. Kay, L. E. (1995) Pulsed field gradient multi-dimensional NMR methods for the study of protein structure and dynamics in solution. *Prog. Biophys. Mol. Biol. 63*, 277–299.
21. Delaglio, F., Grzesiek, S., Vuister, G. W., Zhu, G., Pfeifer, J., and Bax, A. (1995) Nmrpipe: A Multidimensional Spectral Processing System Based On Unix Pipes. *J. Biomol. NMR 6*, 277–293.
22. Johnson, B. A., and Blevins, R. A. (1994) Nmr View: A Computer-Program For the Visualization and Analysis of NMR Data. *J. Biomol. NMR 4*, 603–614.
23. Ottiger, M., Delaglio, F., and Bax, A. (1998) Measurement of J and dipolar couplings from simplified two-dimensional NMR spectra. *J. Magn. Reson. 131*, 373–378.
24. Hansen, M. R., Mueller, L., and Pardi, A. (1998) Tunable alignment of macromolecules by filamentous phage yields dipolar coupling interactions. *Nat. Struct. Biol. 5*, 1065–1074.
25. Brunger, A. T., Adams, P. D., Clore, G. M., DeLano, W. L., Gros, P., Grosse-Kunstleve, R. W., Jiang, J. S., Kuszewski, J., Nilges, M., Pannu, N. S., Read, R. J., Rice, L. M., Simonson, T., and Warren, G. L. (1998) Crystallography & NMR system: A new software suite for macromolecular structure determination. *Acta Crystallogr. D54*, 905–921.
26. Battiste, J. L., and Wagner, G. (2000) Utilization of site-directed spin labeling and high-resolution heteronuclear nuclear magnetic resonance for global fold determination of large proteins with limited nuclear overhauser effect data. *Biochemistry 39*, 5355–5365.
27. Marti-Renom, M. A., Stuart, A. C., Fiser, A., Sanchez, R., Melo, F., and Sali, A. (2000) Comparative protein structure modeling of genes and genomes. *Annu. Rev. Biophys. Biomol. Struct. 29*, 291–325.
28. Dominguez, C., Boelens, R., and Bonvin, A. (2003) HADDOCK: A protein-protein docking approach based on biochemical or biophysical information. *J. Am. Chem. Soc. 125*, 1731–1737.
29. van Dijk, A. D. J., Fushman, D., and Bonvin, A. (2005) Various strategies of using residual dipolar couplings in NMR-driven protein docking: Application to Lys48-linked Di-ubiquitin and validation against N-15-relaxation data. *Proteins: Struct., Funct., Bioinf. 60*, 367–381.
30. Prestegard, J. H., Al-Hashimi, H. M., and Tolman, J. R. (2000) NMR structures of biomolecules using field oriented media and residual dipolar couplings. *Q. Rev. Biophys. 33*, 371–424.
31. Hus, J. C., Marion, D., and Blackledge, M. (2001) Determination of protein backbone structure using only residual dipolar couplings. *J. Am. Chem. Soc. 123*, 1541–1542.
32. Fowler, C. A., Tian, F., Al-Hashimi, H. M., and Prestegard, J. H. (2000) Rapid determination of protein folds using residual dipolar couplings. *J. Mol. Biol. 304*, 447–460.
33. Hus, J. C., Marion, D., and Blackledge, M. (2000) De novo determination of protein structure by NMR using orientational and long-range order restraints. *J. Mol. Biol. 298*, 927–936.
34. Delaglio, F., Kontaxis, G., and Bax, A. (2000) Protein structure determination using molecular fragment replacement and NMR dipolar couplings. *J. Am. Chem. Soc. 122*, 2142–2143.
35. Rohl, C. A., and Baker, D. (2002) De novo determination of protein backbone structure from residual dipolar couplings using rosetta. *J. Am. Chem. Soc. 124*, 2723–2729.
36. Pawson, T., and Schlessinger, J. (1993) Sh2 and Sh3 Domains. *Curr. Biol. 3*, 434–442.
37. Hoeller, D., Crosetto, N., Blagoev, B., Raiborg, C., Tikkanen, R., Wagner, S., Kowanetz, K., Breitling, R., Mann, M., Stenmark, H., and Dikic, I. (2006) Regulation of ubiquitin-binding proteins by monoubiquitination. *Nat. Cell Biol. 8*, 163–169.
38. Clore, G. M., and Garrett, D. S. (1999) R-factor, free R, and complete cross-validation for dipolar coupling refinement of NMR structures. *J. Am. Chem. Soc. 121*, 9008–9012.

BI800439T